Influence of light and temperature on the marine iron cycle: From theoretical to global modeling.

Alessandro Tagliabue, Laurent Bopp, Olivier Aumont, Kevin R. Arrigo

Influence of light and temperature on the marine iron cycle: From theoretical to global modeling

Alessandro Tagliabue,[1,2] Laurent Bopp,[2] Olivier Aumont,[3] and Kevin R. Arrigo[1]

Received 14 March 2008; revised 12 February 2009; accepted 6 March 2009; published 9 June 2009.

[1] Iron regulates net primary production (NPP) in a number of ocean regions and exists in a variety of different forms in seawater, not all of which are bioavailable. We used a relatively complex iron cycle model to examine variability in iron speciation as a function of irradiance/temperature and parameterize its first-order impact in a global ocean biogeochemistry model (OBM), which necessitated certain assumptions regarding the representation of iron chemistry. Overall, we find that higher irradiance (typical of shallower mixed layers) promotes the conversion of dissolved iron (dFe) into bioavailable forms (bFe) and increases bFe concentration by 5–53%, depending on parameter values. Temperature plays a secondary role in controlling bFe, with cold mixed layers increasing bFe concentrations. For a given irradiance and temperature, the presence of bioavailable Fe ligands increases bFe/dFe. When bioavailable Fe ligands are present, then reducing the photolability, increasing the log conditional stability, or increasing the concentration of such ligands all act to increase bFe/dFe. Such processes are currently not represented in global OBMs, where iron is typically parameterized as one pool, and we find that NPP can vary by >±20% regionally if the impact of temperature and irradiance on bFe is included, even under a constant circulation. Additionally, iron chemistry is important in controlling the depth over which phytoplankton iron limitation can be alleviated and the subsequent efficiency of iron-based NPP. We also suggest organically complexed dFe must be bioavailable if distributions of phytoplankton biomass and macronutrients are to be reconciled with observations. Our results are important in understanding the role of the irradiance/mixing regime in governing the supply of iron to phytoplankton under a changing climate. New data sets on iron speciation and rate processes will aid in refining our model.

Citation: Tagliabue, A., L. Bopp, O. Aumont, and K. R. Arrigo (2009), Influence of light and temperature on the marine iron cycle: From theoretical to global modeling, *Global Biogeochem. Cycles*, *23*, GB2017, doi:10.1029/2008GB003214.

1. Introduction

[2] *Sverdrup* [1953] demonstrated that for phytoplankton to bloom, the mixed layer must be shallower than the depth at which vertically integrated photosynthesis is balanced by community respiration (the so-called critical depth). In temperate zones, the onset of stratification is driven by the springtime warming of surface waters, and if this follows a period of deep mixing, then ample macronutrients will be present in the mixed layer to fuel high rates of net primary production (NPP). In polar waters, the formation of sea ice during the austral autumn and winter will drive convective overturn, thus replenishing surface waters with dissolved nutrients. The springtime melting of seasonal sea ice results in the intense stratification of surface waters (due to freshwater input) and very cold, shallow mixed layers that are exposed to high light levels.

[3] However, there are some areas of the worlds oceans where phytoplankton fail to bloom, even under well-stratified conditions with high macronutrient concentrations. Phytoplankton in these "high-nutrient low-chlorophyll" (HNLC) regions are generally limited by the availability of iron (Fe) and such regions include the subarctic Pacific [*Tsuda et al.*, 2003; *Boyd et al.*, 2004], the equatorial Pacific [*Coale et al.*, 1996], and the Southern Ocean [*Boyd et al.*, 2000; *Coale et al.*, 2005]. The Southern Ocean is by far the largest HNLC region, both in terms of geographic area and the abundance of unused macronutrients [*Conkright et al.*, 1994]. Accordingly, it has been proposed that Fe-driven variability in Southern Ocean NPP might contribute to the glacial-interglacial variability in atmospheric CO_2 [*Martin*, 1990]. Additionally, the Fe-limited equatorial Pacific region is also a large source of CO_2 to the atmosphere [*Takahashi et al.*, 2002] and Fe mediated variability in NPP will impact the air-sea pCO_2 gradient.

[1]Department of Geophysics, Stanford University, Stanford, California, USA.
[2]Laboratoire des Sciences du Climat et de l'Environnement, IPSL, CEA, UVSQ Orme des Merisiers, CNRS, Gif sur Yvette, France.
[3]Laboratoire d'Océanographie et de Climatologie: Expérimentation et Approches Numériques, IRD, IPSL, Plouzane, France.

0886-6236/09/2008GB003214

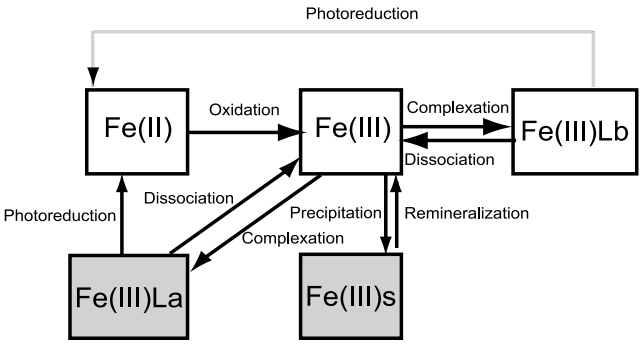

Figure 1. A schematic of the Fe supply model used in this study. All pools shaded white are assumed to be bioavailable forms of Fe (bFe). Processes present in all incarnations of the model are represented by black arrows, while photoreduction of bioavailable organically complexed Fe (Fe(III)Lb) is not always present and is represented by a gray arrow.

[4] The cycle of Fe in seawater is complex and the speciation, and thus bioavailability, of Fe is controlled by both physical and biological factors [*Morel and Price*, 2003]. While nominally available to phytoplankton, Fe′ (defined as the sum of free inorganic Fe(II) and Fe(III)) typically only exists at picomolar levels in oxygenated seawater, with >99% of dissolved Fe (dFe) complexed by a variety of organic ligands [*Gledhill and van den Berg*, 1994]. Traditionally, only uncomplexed "free" inorganic Fe was thought to be available for phytoplankton uptake (the Fe′ model) [*Hudson and Morel*, 1990], which is controlled by ligand kinetics and photochemistry. However, recent field and laboratory research has shown that at least some portion of the organically complexed Fe pool is likely to be available to phytoplankton [e.g., *Hutchins et al.*, 1999; *Maldonado and Price*, 2001; *Blain et al.*, 2004; *Maldonado et al.*, 2005, 2006], although its ubiquity and the precise mechanisms employed remain a matter of debate [*Hutchins et al.*, 1999; *Blain et al.*, 2004; *Shaked et al.*, 2005; *Maldonado et al.*, 2005, 2006; *Salmon et al.*, 2006]. Fe(II) oxidation can be represented as a first-order function of temperature [*Millero et al.*, 1987] while the resupply of Fe(II) via photoreduction is mediated by irradiance [*Barbeau et al.*, 2001; *Emmenegger et al.*, 2001; *Rijkenberg et al.*, 2005] and can result in a buildup of Fe(II) in surface waters [*Croot et al.*, 2001; *Bowie et al.*, 2002; *Tagliabue and Arrigo*, 2006]. Any uncomplexed Fe(III) is converted to nonbioavailable forms via precipitation/scavenging.

[5] While the importance of Fe to phytoplankton physiology is relatively well established [e.g., *Raven*, 1988; *Sunda and Huntsman*, 1997], the impact of the irradiance/mixing regime on Fe bioavailability and cycling is less well understood. For example, temperature will impact phytoplankton growth rates [*Eppley*, 1972], as well as rates of Fe oxidation [*Millero et al.*, 1987], while light controls the rate of photosynthesis [*Ryther*, 1956], the carbon-specific Fe demand [*Raven*, 1988], and the photoreduction of organically complexed Fe [*Barbeau et al.*, 2003]. Current generation of global ocean biogeochemistry models (OBMs) only account for Fe speciation in a simplistic manner and neglect the impact of abiotic processes on Fe bioavailability [e.g., *Gregg et al.*, 2003; *Dutkiewicz et al.*, 2005; *Aumont and Bopp*, 2006; *Moore and Doney*, 2007]. Nevertheless, a recent regional study of Fe speciation within a 3D ecosystem model of the Ross Sea (Antarctica) demonstrated that abiotic processes increased bFe in shallow mixed layers and elevated the efficiency with which dFe could fuel NPP [*Tagliabue and Arrigo*, 2006]. Additionally, *Weber et al.* [2007] recently employed a similar Fe speciation model in a 1D NPZD model framework at the Bermuda Atlantic Time-series, but did not focus on Fe speciation within the dFe pool and its impact on bioavailability (only Fe(III) was assumed bioavailable).

[6] In this study, we extended the work of *Tagliabue and Arrigo* [2006] to examine the cycling and supply of bioavailable Fe (bFe) for a suite of irradiance and temperature regimes (tropical, temperate, and polar conditions) with the goal of including variability in bFe within a global OBM and addressing the debate on Fe acquisition strategies. We were interested in (1) generalizing the relationship between bFe and light and temperature under a variety of assumptions regarding the speciation and photolability of bFe, (2) accounting for Fe speciation in a global OBM, (3) evaluating its impact under an unchanging circulation, and (4) using the new OBM to investigate the likelihood that only inorganic Fe is bioavailable (the traditional Fe′ model). Environmentally driven variability in Fe chemistry has not been considered previously, yet may be critical in governing the response of HNLC ecosystems to a changing circulation, as well as phytoplankton growth rates in Fe-poor waters.

2. Methods

2.1. Offline Fe Supply Model

[7] As we were interested in examining the role of the irradiance/mixing regime in governing Fe cycling and speciation, we used the Fe supply model of *Tagliabue and Arrigo* [2006], ignoring the role of biological processes. The standard abiotic Fe cycle model consists of five Fe pools, including four dissolved (dFe) and one solid (Fe(III)s) pool (Figure 1). The dFe pools consist of two free inorganic pools (Fe(II) and Fe(III)) and two ligand-bound Fe(III) pools, one of which is nonbioavailable, but photolabile (Fe(III)La) while the other is bioavailable (Fe(III)Lb, and may or may not be photolabile; we will investigate both scenarios). The remaining Fe pool consists of Fe(III) that has precipitated to form solid Fe(III)s. We have made assumptions regarding the characteristics of seawater Fe ligands and their bioavailability and follow available literature estimates regarding the values assigned to abiotic rate processes (see below).

[8] Inorganic Fe(II) is oxidized to Fe(III) via a pseudo-first-order rate constant (k_{ox}) that is a function of temperature [*Millero et al.*, 1987], including the low-temperature Fe(II) half lives measured during the Southern Ocean Iron Enrichment Experiment (SOIREE) [*Bowie et al.*, 2001]. We acknowledge that the short half-life of Fe(II) in oxygenated seawater can make in situ measurements a challenge as the

Table 1. Values for the Rate Constants[a]

T	k_{ox}	E	k_{pr}
−5	7.92×10^{-5}	0	0
0	1.64×10^{-4}	10	4.77×10^{-6}
5	3.39×10^{-4}	20	9.54×10^{-6}
10	7.02×10^{-4}	30	1.43×10^{-5}
15	1.45×10^{-3}	40	1.91×10^{-5}
20	3.01×10^{-3}	50	2.39×10^{-5}
25	6.23×10^{-3}	70	3.34×10^{-5}

[a]For Fe(II) oxidation (k_{ox}, s^{-1}) and Fe(III)La photoreduction (k_{pr}, s^{-1}) for the range of temperatures (T, °C) and irradiances (E, W m^{-2}) used in this study.

redox speciation may change following oxidation to Fe(III) and subsequent precipitation as oxyhydroxides. We assume that Fe(III)La complexes are photolabile and can be photoreduced to produce Fe(II), via ligand-to-metal charge transfer [*Barbeau et al.*, 2001], at rates that are a function of the incident PAR [*Rijkenberg et al.*, 2005]. Although photoreduction appears to be lower (per quantum) for PAR than for UV (not included in this study), most all measured photoreduction has typically been ascribed to PAR [*Rijkenberg et al.*, 2005; *Maldonado et al.*, 2005], which is much more abundant than UV radiation. Indeed, numerous experiments measuring photoreduction by natural sunlight used polycarbonate bottles that excluded UV radiation [e.g., *Barbeau et al.*, 2001; *Maldonado et al.*, 2005].

[9] The rate of change in Fe(II) (μmol m^{-3} s^{-1}) is

$$Q_{Fe(II)} = -k_{ox}Fe(II) + k_{pr}Fe(III)La + k_{prLb}Fe(III)Lb \quad (1)$$

and the rate of change in Fe(III) (μmol m^{-3} s^{-1}) is

$$\begin{aligned} Q_{Fe(III)} = {} & k_{ox}Fe(II) - k_{fFe(III)La}Fe(III)[La] + k_{dFe(III)La}Fe(III)La \\ & - k_{fFe(III)Lb}Fe(III)[Lb] + k_{dFe(III)Lb}Fe(III)Lb \\ & - k_{pcp}Fe(III) + R_{Fe(III)s}Fe(III)s \end{aligned} \quad (2)$$

where Fe(III) is produced by oxidation of Fe(II) (k_{ox}Fe(II)) and is lost by precipitation to Fe(III)s (k_{pcp}Fe(III)). Rate constants for the formation (4.2×10^4 M^{-1} s^{-1}) and dissociation (2×10^{-7} s^{-1}) of Fe(III)La (to yield a log conditional stability constant of 11.32 M^{-1}) are taken from measurements of *Witter and Luther* [1998]. *Maldonado et al.* [2005] demonstrated significant in situ phytoplankton uptake of Fe-ligand complexes with kinetic characteristics that were similar to desferroxamine (DFO) ligands in the Fe-limited Southern Ocean. We therefore ascribe rate constants for the formation (19.6×10^5 M^{-1} s^{-1}) and dissociation (1.5×10^{-6} s^{-1}) of Fe(III)Lb (to yield a log conditional stability constant of 12.12 M^{-1}) in accordance with the measured kinetics of DFO [*Witter et al.*, 2000] and assume that Fe(III)Lb complexes are photostable [*Barbeau et al.*, 2003] (we explore the sensitivity to these assumptions later). This agrees well with the measurements in the Atlantic Ocean of low-concentration ligands with log conditional stability constants of between 12 to 13 M^{-1} and a higher-concentration ligand typified by a weaker log conditional stability constant of around 11 M^{-1} [*Cullen et al.*, 2006]. The concentrations of La and Lb are set to 2 nM and 0.6 nM (Fe equivalents), respectively.

[10] The rate of change in Fe(III)La (μmol m^{-3} s^{-1}) is modeled as

$$\begin{aligned} Q_{Fe(III)La} = {} & k_{fFe(III)La}Fe(III)[La] \\ & - k_{dFe(III)La}Fe(III)La - k_{pr}Fe(III)La \end{aligned} \quad (3)$$

where Fe(III)La can be photoreduced (k_{pr}Fe(III)La) to form Fe(II) and thermodynamically dissociates to Fe(III) ($k_{dFe(III)La}$Fe(III)La). Fe(III)La complex formation is as described above.

[11] The rate of change in Fe(III)Lb (μmol m^{-3} s^{-1}) is

$$\begin{aligned} Q_{Fe(III)Lb} = {} & k_{fFe(III)Lb}Fe(III)[L_b] \\ & - k_{dFe(III)Lb}Fe(III)Lb - k_{prLb}Fe(III)Lb \end{aligned} \quad (4)$$

where Fe(III)Lb is formed as per Fe(III)La and is lost via thermodynamic dissociation ($k_{dFe(III)Lb}$Fe(III)Lb). When Lb is assumed to be photolabile, photoreduction (k_{prLb}Fe(III)Lb) is an additional loss of Fe(III)Lb and source of Fe(II). The rate constant for photoreduction of Fe(III)Lb (k_{prLb}) is assumed to be the same as for Fe(III)La (in the absence of any ligand-specific information). On the other hand, if we assume that Fe(III)Lb complexes are photostable, then k_{prLb} is assumed to be zero.

[12] Fe(III)s is produced via precipitation/scavenging of Fe(III) (k_{pcp}Fe(III)) and is remineralized back to Fe(III) at a rate of 0.05 d^{-1}. Therefore, the rate of change in Fe(III)s (μmol m^{-3} s^{-1}) is simply

$$Q_{Fe(III)s} = k_{pcp}Fe(III) - R_{Fe(III)s}Fe(III)s \quad (5)$$

and does not include sinking. For reference, we include the rate constants for Fe(II) oxidation and Fe(III)La photoreduction (k_{ox} and k_{pr}, respectively, s^{-1}) in Table 1.

2.2. Model Experiments

[13] Quasi-equilibrium model simulations were conducted under a range of mixed layer irradiances (0 to 75 W m^{-2}) and temperatures (−5 to 25°C, with −5 used to provide a "lower bound") by running the model at a time step of 1 s for >200 days (to ensure equilibration). The total Fe pool is fixed at 0.5 nM and reflects typical oceanic concentrations in HNLC regions [e.g., *Johnson et al.*, 1997; *Coale et al.*, 2005]. dFe includes Fe(II), Fe(III), Fe(III)La, and Fe(III)Lb, bFe is assumed to be Fe(II), Fe(III) and Fe(III)Lb, while total Fe (tFe) is dFe + Fe(III)s. Fe′ is defined as the sum of the free inorganic Fe species (Fe(II) and Fe(III)). Rather than the absolute Fe concentrations, we were interested in appraising the proportion of the total Fe pool present as dissolved Fe (dFe/tFe), the proportion of the dFe pool present as bFe (bFe/dFe), as well as the proportion of the dFe pool present as Fe(II) (Fe(II)/dFe).

[14] In our standard case, we assume Lb is present and photostable with the kinetic characteristics of DFO [*Witter et al.*, 2000]. We conducted four major sensitivity tests during our investigations. First, we assumed there was no Lb and only inorganic Fe is bioavailable, i.e., conforming to

the Fe′ model of bioavailability. Second, we examined the impact of assuming Lb is photolabile (i.e., k_{prLb} in equation (4) is not zero). Third, we studied the impact of different Lb concentrations (the concentration of Lb was halved and doubled). Fourth, the log conditional stability of Fe(III)Lb complexes was increased to 12.34 M^{-1} (by decreasing both the formation and dissociation rate constants as per phytic acid) and decreased to 11.00 M^{-1} (by increasing the dissociation rate constant as per phaeophytin). Modifications to the ligand kinetics followed measurements of phytic acid and phaeophytin ligands [*Witter et al.*, 2000].

2.3. Model Caveats

[15] In this study we did not include the cycling of either hydrogen peroxide (H_2O_2) or superoxide (O_2^-). The cycling of both compounds are also controlled by photochemical processes and can be involved in the oxidation of Fe(II) and the back reduction of Fe(III) [*King et al.*, 1995]. While any irradiance-driven maxima in photochemical radicals could enhance Fe(II) production from Fe(III) (further increasing bFe), it should be noted that free Fe(III) concentrations were extremely low during our simulations (always <4 pM), with most Fe(III) present as either organic complexes or precipitates (Fe(III)s in our notation). Moreover, H_2O_2 and O_2^- are also involved in the redox cycle of copper (Cu) [*Zafiriou et al.*, 1998] and since Cu is likely to be involved in the phytoplankton uptake of organically bound Fe [*Maldonado et al.*, 2006], the inclusion of such features is by no means straightforward.

[16] Our model is similar to that of *Weber et al.* [2007] in many respects, but is employed to address the role of abiotic processes in governing bFe. Notable differences in the *Weber et al.* [2007] model include the presence of H_2O_2 and O_2^-, but without a link to the availability of organically complexed Fe (in the sense of *Maldonado et al.* [2006]), and the inclusion of an Fe(III) colloidal pool (that is assumed to be "dissolved"). In our study, we assume Fe(III) contains both "free inorganic" species and colloids <0.2 μm in diameter, and assume both can be complexed by organic ligands and all uncomplexed Fe(III) can precipitate and be scavenged by particles. It is important to note that the model of *Weber et al.* [2007] assumes that only free inorganic Fe(III) is available for phytoplankton uptake (i.e., conforming to the Fe′ uptake model [*Hudson and Morel*, 1990]), despite evidence to the contrary [e.g., *Hutchins et al.*, 1999; *Maldonado and Price*, 2001; *Blain et al.*, 2004; *Maldonado et al.*, 2005, 2006] and that >99% of dFe is typically organically complexed. We will explore the importance of such an assumption during this study and the global impact of assuming only inorganic Fe is bioavailable.

2.4. PISCES Global Ocean Biogeochemistry Model

[17] The Pelagic Integration Scheme for Carbon and Ecosystem studies (PISCES) global OBM is fully described by *Aumont and Bopp* [2006]. In brief, PISCES includes two phytoplankton functional groups (nanophytoplankton and diatoms), mesozooplankton and microzooplankton, 2 detrital size classes, calcium carbonate, dissolved inorganic carbon, carbonate, dissolved organic carbon, nitrate (NO_3), phosphate (PO_4), Silicic acid ($Si(OH)_4$), and iron (Fe) [*Aumont and Bopp*, 2006]. Fixed "Redfield ratios are employed for NO_3 and PO_4, while the Si/C and Fe/C ratios vary dynamically as a function of the phytoplankton functional group and environmental conditions. Fe/C ratios increase with decreasing light (due a greater physiological Fe demand) and increasing concentrations of Fe (due to the upregulation of cellular processes that require Fe). At a given concentration of Fe, diatoms are assumed to be more strongly limited and have a greater Fe demand than nanophytoplankton. PISCES is a good candidate with which to explore the significance of representing Fe chemistry as it has been evaluated/employed for a wide range of biogeochemical studies [e.g., *Aumont and Bopp*, 2006, *Tagliabue and Bopp*, 2008; *Tagliabue et al.*, 2008], including those concerned with interannual variability [*Rodgers et al.*, 2008; *Schneider et al.*, 2008] and future climate [*Bopp et al.*, 2005].

[18] PISCES also does a good job of representing global ocean dFe concentrations [*Tagliabue et al.*, 2008]. In surface waters, monthly correlation coefficients (R, after log transformation) range between 0.41 (in October) and 0.79 (in August), with a mean of 0.61. In subsurface (100 and 300 m) and deep (2000 and 3000 m) waters, R is 0.63 and 0.77, respectively. Root mean squared errors (RMSE) for dFe are 0.47, 0.35 and 0.30 for depths of 0 to 50 m, 100 to 300 m, and 2000 to 3000 m, respectively. For comparison, the recent global OBM of *Moore and Braucher* [2007] reports R and RMSE values for dFe concentrations (log transformed) of 0.598 and 0.443, and 0.602 and 0.338 for depth ranges of 0 to 103 m and 103 to 502 m, respectively.

2.5. Representing Fe Chemistry in PISCES

[19] We are able to include the first-order effect of light and temperature on bFe in the PISCES OBM. Prognostically simulating the five Fe pools used in this study at the necessary short time step is possible in a regional 3D biogeochemical model [*Tagliabue and Arrigo*, 2006], but remains computationally prohibitive in a global OBM. However, we can use results of our abiotic model to generate a lookup table of bFe/dFe for a given range of irradiances and temperatures (we chose the results from the photolabile ligand scenario presented in Figure 2h, which agrees with field observations on ligand photolability, as well as generating realistic Fe(II)/dFe predictions, see section 3.3). This enables us to determine the bFe concentration from the dFe concentration, irradiance, and temperature variables that are already simulated by PISCES.

3. Results and Discussion

3.1. Sensitivity Tests With the Fe Supply Model

3.1.1. Photostable Bioavailable Ligand

[20] Beginning with our standard case, a photostable bioavailable ligand (Lb) all but eliminates nonbiogenic losses of dFe and results in bFe making up a greater proportion of dFe as irradiance increases (Figures 2a and 2b). Over 99.9% of Fe is complexed by either La or Lb across the full range of irradiances (i.e., dFe $\cong$ tFe, Figure 2a). Although increased light elevates the photoproduction of inorganic Fe from

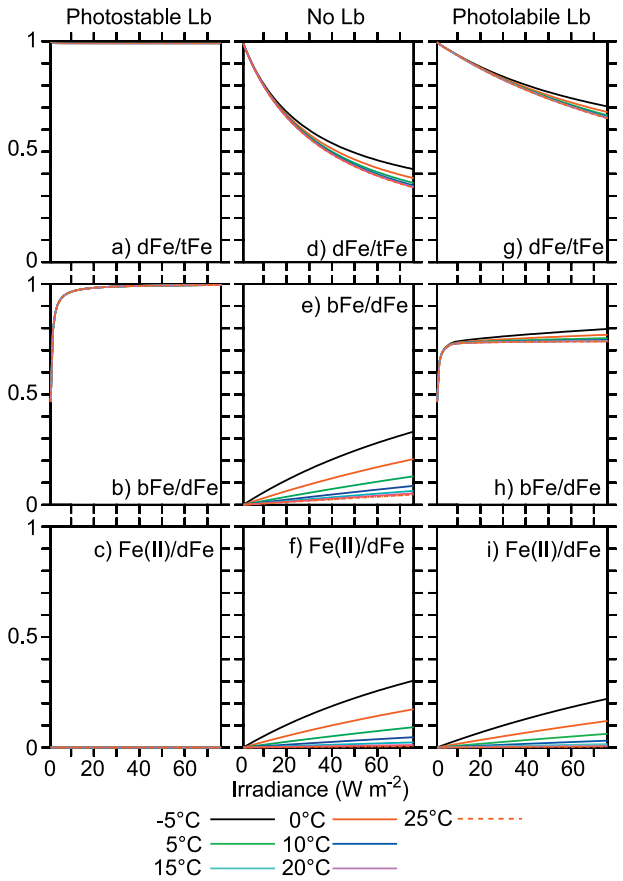

Figure 2. Impacts of changes in irradiance and temperature on the proportion of tFe present as dFe (dFe/tFe), the proportion of dFe present as bFe (bFe/dFe), and the proportion of dFe present as Fe(II) (Fe(II)/dFe) for the offline Fe supply model, assuming that bioavailable Fe ligands are either (a–c) present and photostable, (d–f) absent, or (g–i) present and photolabile. Note that there is no temperature sensitivity in Figures 2a–2c.

Fe(III)La (Table 1), it is rapidly complexed by the photostable Lb to form Fe(III)Lb and the losses of dFe and accumulation of Fe(II) are negligible (Figures 2a and 2c). This also results in little sensitivity to temperature. Nevertheless, since bFe/dFe is lower in the dark, light is important in providing a means by which the dFe pool can be mobilized and complexed by Lb, thereby increasing bFe/dFe by over 50% across our range of irradiances (Figure 2b).

3.1.2. No Bioavailable Ligand

[21] If Lb is absent, then bFe/dFe declines significantly, relative to our standard case, but still increases with light. During this scenario, bFe is assumed to be made up only of free inorganic Fe(II) and Fe(III) and reflects the traditional Fe′ model of phytoplankton Fe uptake [*Hudson and Morel*, 1990]. Since Lb is no longer present to buffer bFe concentrations (bFe = Fe′), dFe/tFe declines and bFe/dFe is reduced drastically (by over 50% relative to the photostable bioavailable ligand case, Figures 2d and 2e). That said, photochemistry still results in greater bFe/dFe at high light levels, although the temperature dependency of Fe(II) residence times (Table 1) reduces Fe(II)/dFe, and thus bFe/dFe, in warm waters (Figures 2e and 2f). Indeed, if there are no bioavailable Fe ligands present, it appears that bFe (i.e., free inorganic Fe) can only approach 10% of the dFe pool only in cold and well lit mixed layers (Figure 2e). This is likely to have implications for the viability of the Fe′ uptake model in warm waters, even if they are well lit. Since any free Fe(III) is either complexed by the nonbioavailable ligand (La) or lost as Fe(III)s, most of this bFe is present as Fe(II) (Figure 2f).

3.1.3. Photolabile Bioavailable Ligand

[22] Assigning photolability to Fe(III)Lb reduces bFe/dFe, relative to the standard case, and results in a greater sensitivity to temperature. Fe(III)Lb is more labile when photoreduction is an additional loss and the increased turnover of Fe at high light levels drives greater nonbiogenic losses of dFe (as Fe(III)s) and reduces dFe/tFe (by up to 20% at very high irradiances; Figure 2g). On the other hand, the photoreduction of Fe(III)Lb results in a significant proportion of dFe being present as Fe(II) (up to 20% at the highest light and coldest temperatures; Figure 2i). Although bFe/dFe is reduced, it remains much greater than when Lb was absent and increases with irradiance (Figure 2h). Field observations by *Maldonado et al.* [2006] suggest that bioavailable organically complexed Fe in the Southern Ocean was likely to be photolabile. The photolability of Fe ligands depends on the functional moiety of the Fe binding group and typically requires an α-hydroxy acid group [*Barbeau et al.*, 2003]. In seawater, a currently limited data set suggests that α-hydroxy acid groups are present in situ, but typically occur alongside hydroxamate and catecholate groups as mixed moiety ligands [*Reid et al.*, 1993; *Martinez et al.*, 2000, *Barbeau et al.*, 2001; *Macrellis et al.*, 2001].

3.1.4. Bioavailable Ligand Concentration

[23] The ratios of bFe/dFe and dFe/tFe were proportional to the concentration of Lb, with changes being greater when Fe(III)Lb was photolabile. It is noteworthy that the concentration of Lb is important in setting the intercept of the bFe/dFe relationship (Figure S1), which would relate to the bFe/dFe value in deep waters.[1] Recent work has shown that there is a wide degree of variability in oceanic ligand concentrations, especially in coastal waters and a consistently positive correlation between the concentrations of ligands and dFe is observed across a wide variety of ocean systems (see the compilation given by *Buck and Bruland* [2007]). We also find that dFe/tFe is elevated when ligand concentrations are higher and we would suggest that there should also be a concomitant increase in Fe bioavailability (Figure S1). While constraining the sources of Fe binding ligands in seawater remains speculative, their role in controlling the concentration of dFe [*Buck and Bruland*, 2007; *Buck et al.*, 2007; this study], and possibly also bFe (this study), highlights the need for more information on their sources and sinks in order to better model this variability.

3.1.5. Bioavailable Ligand Kinetics

[24] While changing the kinetics of Lb does change the absolute values associated with bFe/dFe and Fe(II)/dFe, the

[1] Auxiliary materials are available in the HTML. doi:10.1029/2008GB003214.

positive trends with irradiance are robust. Unsurprisingly, reducing the log conditional stability constant reduces bFe/dFe and dFe/tFe, but increases Fe(II)/dFe (Figure S2). Reducing the formation and dissociation rate constants, but slightly increasing the overall log conditional stability constant, slightly reduces dFe/tFe and bFe/dFe, with little change in Fe(II)/dFe (Figure S2). As seen previously, these trends are exacerbated when Fe(III)Lb is photolabile. Nevertheless, bFe/dFe increases with light, with temperature only playing a secondary role.

3.2. Generalized Relationship Between bFe and Light and Temperature

[25] Regardless of how we chose to parameterize bFe or the kinetic/photochemical characteristics of Lb in our Fe cycle model, we found that the proportion of the dFe pool present as bFe increases with greater irradiance. We tested 3 fundamental assumptions regarding bioavailable Fe ligands (present and photostable, present and photolabile, and absent), as well as 3 different concentrations and kinetic characteristics of Lb, and found a consistent positive trend in bFe/dFe with respect to irradiance (Figures 2b, 2e, and 2h). The increase in bFe/dFe can be as great as 53% (when Lb is present and photostable across all temperatures), or as low as 5% (when Lb is absent at 25°C) and is dependent on bioavailability assumptions and the mixed layer temperature. If the ligand pool has a high lability, or is absent, then there is also an inverse relationship between bFe/dFe and temperature (but this is a second-order effect relative to the role of irradiance). Overall, this would suggest that the ocean bFe pool is highly dynamic and responds to variability in abiotic processes that are mediated by the irradiance/mixing regime of surface waters, in addition to any changes in exogenous Fe inputs. For example, the increase in irradiance that is associated with the springtime stratification of the mixed layer will not only impact phytoplankton photosynthesis (as noted by *Sverdrup* [1953]), but will also promote the conversion of Fe to bioavailable forms. Accordingly, abiotically controlled increases in bFe can contribute to the elevated primary productivity of stratified offshore HNLC regions [*Moore and Doney*, 2006] or the greater efficiency of mesoscale Fe fertilization experiments in shallow mixed layers [*de Baar et al.*, 2005]. In general, for a given irradiance and temperature, the presence of bioavailable Fe ligands increases bFe/dFe, and if bioavailable Fe ligands are already present, then reducing their photolability, increasing their log conditional stability, or increasing their concentration all act to increase bFe/dFe.

3.3. Measurements to Test Fe Models

[26] As in situ measurements of bFe will require new and innovative investigations, Fe(II) might provide a potential means to assess the importance and nature of abiotic Fe cycling. Recent advances have permitted the shipboard determination of seawater Fe(II) concentrations [*King et al.*, 1995; *Bowie et al.*, 2002; *Croot and Laan*, 2002; *Boye et al.*, 2006], alongside the more typical dFe measurements. In our model experiments, Fe(II)/dFe increases with light and can make up between 0 and 20% of the dFe pool (depending on light and temperature), but remains near zero if bioavailable ligands are assumed photostable. Consistent with these results, measured Fe(II)/dFe ratios were between 0.03 and 0.35 in the Atlantic and Southern Oceans and displayed a positive relationship with irradiance [*Bowie et al.*, 2002; *Boye et al.*, 2006], although *Boye et al.* [2006] noted the potential for biologically mediated production in subsurface layers (a process not present in our model). During SOIREE, relatively high concentrations of Fe(II) persisted for up to 4 days after the final Fe infusion [*Croot et al.*, 2001; *Bowie et al.*, 2001]. Our results suggest that it is possible for photochemistry to maintain appreciable concentrations of Fe(II) in the mixed layer without necessitating the inclusion of Fe(II)-specific ligands (especially in the cold waters of the Southern Ocean; Figure 2f). Overall, we find that predictions of Fe(II)/dFe exhibit a high degree of variability that is connected to the turnover time of the dFe pool and the residence time of Fe(II) (Figures 2e, 2f, and 2i). Future in situ measurements of Fe(II)/dFe, which also address the irradiance/mixing regime, might assist in the appraisal of different Fe cycle formulations. That said, we note the difficulty of making such measurements in oxygenated seawater (see Methods), but are encouraged by recent progress by the GEOTRACES community [*Henderson et al.*, 2007].

3.4. Fe Chemistry in PISCES

3.4.1. Impact of Fe Chemistry

[27] Including Fe chemistry in PISCES causes phytoplankton to be impacted by changes in Fe speciation with depth and permits us to capture the processes driving bFe supply and demand. As such, we find phytoplankton productivity and species composition respond to abiotic processes that drive bFe supply. Although Southern Ocean NPP changes little under an unchanging circulation, we do find a reduction in diatom abundance results (Figure 3). This is because the irradiance driven reduction in bFe concentrations causes diatoms to be less competitive than smaller nanophytoplankton. In the equatorial Pacific, we find predictions of annual net primary production (NPP) to be more sensitive to the inclusion of chemical processes (± 30 g C m^{-2} a^{-1} or $\pm 20\%$), even if there are no changes in circulation. Under a climatologically forced circulation [*Aumont and Bopp*, 2006], equatorial Pacific NPP actually increases if bFe varies with light and temperature (Figure 4). This is despite the fact the bFe concentration (relative to dFe) is reduced, which increases Fe limitation. Accordingly, in the equatorial Pacific region, we find that subsurface bFe concentrations are reduced (Figure 4), because of the lower light levels therein. This indeed reduces the in situ phytoplankton utilization (subsurface NPP declines; Figure 4), but also permits greater quantities of bFe to reach well-lit surface waters. Phytoplankton NPP is more efficient at higher irradiance levels (the Fe/C ratio decreases with light; Figure 4) [*Raven*, 1988], and total NPP therefore increases by more in the surface than it declined in the subsurface. This vertical redistribution of bFe toward well lit surface waters, where it can more efficiently fuel carbon fixation, is exacerbated in upwelling zones, as excess bFe is effectively transported to surface waters. Additionally, the greater bFe supply to surface waters acts to increase diatom abundance over that of nanophytoplankton (Figure 3).

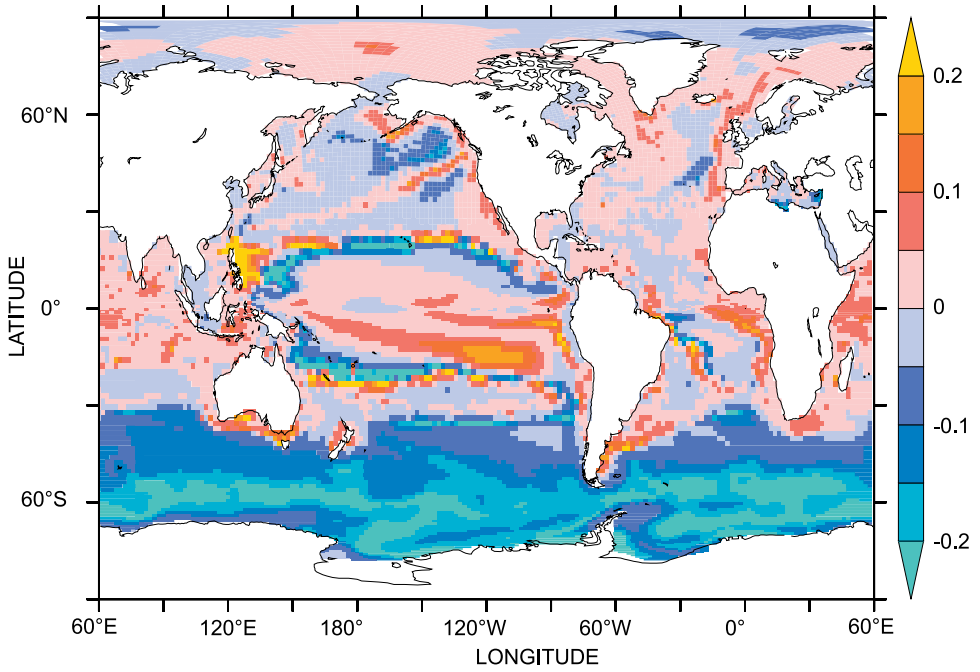

Figure 3. The proportional change in diatom biomass (calculated as the contribution of diatoms to total phytoplankton carbon biomass, no units) between a climatological simulation (i.e., no changes in circulation) where bFe varies as per Figure 2h and an identical simulation where bFe = dFe (i.e., no abiotic variability).

3.4.2. Improving the Realism of PISCES

[28] As well as impacting NPP, including Fe chemistry improves the spatial distribution of equatorial Pacific phytoplankton biomass in PISCES. In the previous version of PISCES [*Aumont and Bopp*, 2006], a minimum Fe threshold (of 0.01nM) was necessary to accurately represent the biogeochemical dynamics of the equatorial Pacific region. If this parameterization is removed, all the Fe that is upwelled in the eastern equatorial Pacific is utilized close to the upwelling sites and the phytoplankton bloom cannot propagate westward (compare Figure 5a with Figures 5b and 5c). Therefore, such a parameterization (which represents an additional, yet unconstrained, Fe source) was deemed necessary to accurately represent the distribution of tropical Pacific chlorophyll *a*, especially in spring, as well as the transition between Fe and NO_3 limitation [see *Aumont and Bopp*, 2006]. Furthermore, simulations with coupled climate models show that interannual variability is poorly represented in models that do not have a minimum Fe threshold, since the degree of Fe limitation is too great [*Schneider et al.*, 2008]. However, it is encouraging that when we include the first-order impact of Fe speciation in PISCES, we are able to represent the zonal extent of equatorial Pacific chlorophyll *a*, without needing to include an unconstrained Fe source (Figure 5d). This suggests that variability in Fe speciation and bioavailability might be an important factor controlling tropical Pacific phytoplankton biomass and perhaps also interannual variability.

3.4.3. Assessing the Importance of Organically Complexed Fe to Phytoplankton

[29] Distributions of NO_3 and phytoplankton chlorophyll biomass from PISCES suggest that it is unlikely that phytoplankton are only limited by inorganic Fe. This is due to the drastic reduction in bFe/dFe if only inorganic Fe is bioavailable (Figure 2e). It is only in waters colder than 0°C that bFe can exceed 10% of the dFe pool, and the degree of Fe limitation, especially in warm waters, is chronic. Accordingly, when we use the predictions of bFe/dFe from Figure 2e to calculate bFe concentrations in PISCES pervasive Fe limitation markedly reduces phytoplankton chlorophyll *a* production and NO_3 uptake and their distributions do not match observations (Figures 6e and 6f). Although phytoplankton biomass (when bFe = Fe′) can increase slightly if the sedimentary and atmospheric sources of Fe are increased tenfold, this results in unrealistically high residual dFe concentrations (Figure 6d). It therefore appears likely that the majority of phytoplankton can access organically complexed iron and the Fe′ model is unlikely to be the dominant form of Fe uptake.

4. Perspectives

4.1. Bioavailable Fe Pools

[30] The ability to access organically complexed Fe may be a common feature of phytoplankton that have a high requirement for Fe, even in cold waters. We find that bioavailable Fe ligands can drastically increase bFe concentrations (Figure 2), which suggests that their production and uptake would be an advantageous growth strategy for phytoplankton growing in HNLC regions. In the field, uptake of organically complexed Fe has been demonstrated in large diatoms from both the subarctic Pacific [*Maldonado and Price*, 1999] and the Southern Ocean [*Maldonado et al.*, 2005] and phytoplankton growth is enhanced in the

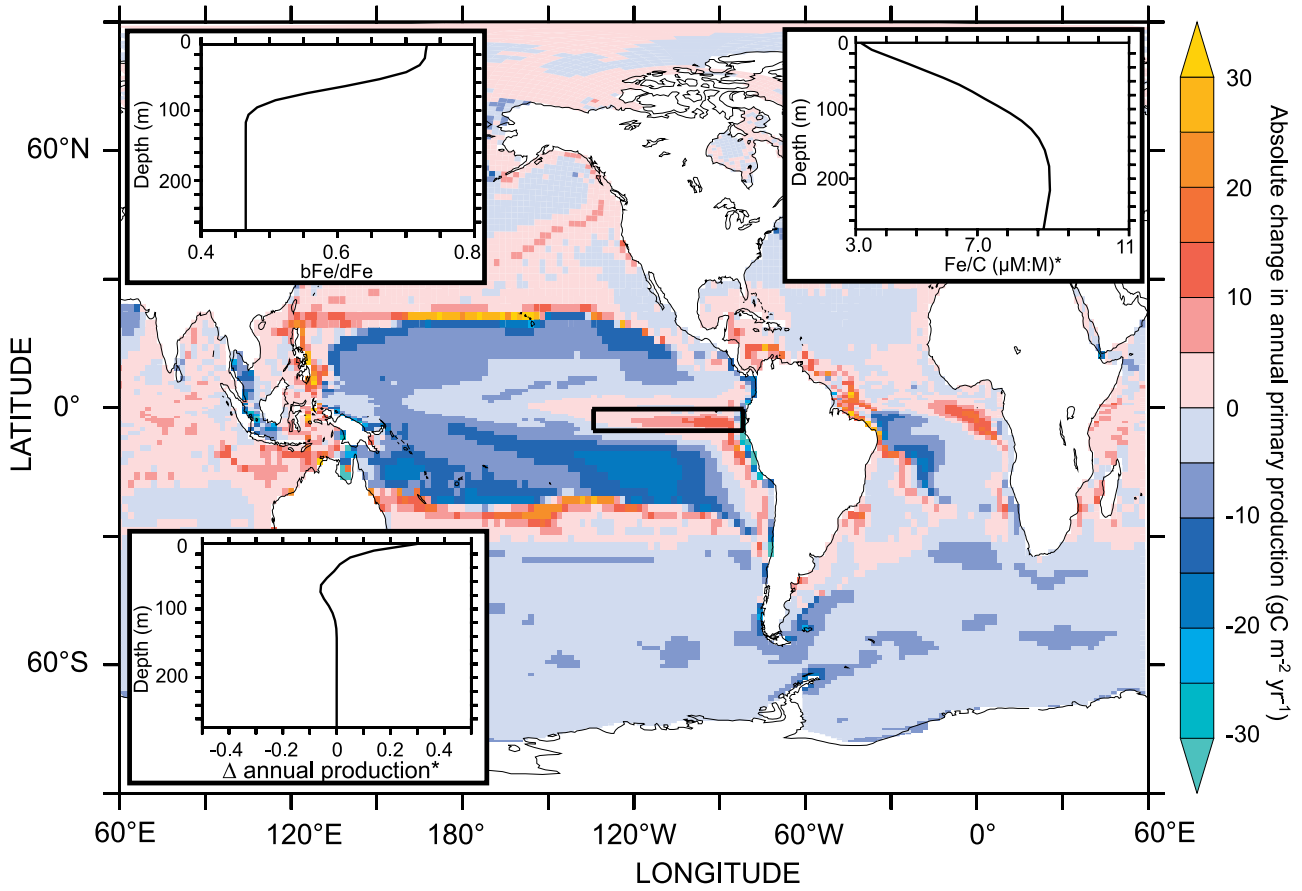

Figure 4. The difference in annual depth integrated NPP (gC m^{-2} a^{-1}) between a climatological simulation (i.e., no changes in circulation) where bFe varies as per Figure 2h and an identical simulation where bFe = dFe (i.e., no abiotic variability). The insets show the vertical variability in the proportion of dFe present as bFe (bFe/dFe, top left), the absolute change in annual NPP (g C m^{-3} a^{-1}, bottom left), and the phytoplankton Fe/C ratio (μM:M, top right) taken from the boxed region of the equatorial Pacific.

presence of organically complexed Fe during incubation experiments [*Ozturk et al.*, 2004], which is suggestive of an increase in bFe. In accord, we find assuming that only inorganic Fe is bioavailable results in unrealistic distributions of NO_3 and chlorophyll *a* when simulated in PISCES (Figures 6e and 6f). The importance of organically complexed Fe to phytoplankton might depend on their affinity for Fe [*Tagliabue and Arrigo*, 2006], which is typically a function of the cell surface area to volume ratio [e.g., *Timmermans et al.*, 2004]. It is therefore reasonable to suggest that large diatoms from the subarctic Pacific and Southern Ocean that take up organically complexed Fe [*Maldonado and Price*, 1999; *Maldonado et al.*, 2005] likely also have a high requirement for Fe. In support of this hypothesis, work in the North Atlantic by *Blain et al.* [2004] demonstrated that the ability of phytoplankton to access organically complexed Fe increased with increasing cell size (and thus a reducing surface area to volume ratio). The bioavailability of Fe bound to distinct ligand types is likely to be dependent on the denticity (the number of ligands minus Fe atom bonds) of the Fe-L complex [*Boukhalfa and Crumbliss*, 2002], as well its age and molecular weight [*Chen et al.*, 2003]. If so, Fe bound to hexdentate ligands, such as DFO, would be less available than Fe bound to the tridentate phytic acid [*Maldonado et al.*, 2005], further highlighting the need for more information regarding the ocean Fe ligand pool (including those that may complex Fe(II) [e.g., *Willey et al.*, 2008]).

4.2. Representing Fe Speciation in Global OBMs

[31] By representing Fe chemistry in the PISCES global OBM, we find that Fe-regulated NPP is more efficient at shallow depths. This is due to the greater bFe supply and reduced bFe demand when irradiance is high. Under a constant circulation, upwelling regions (such as the equatorial Pacific) have a particular sensitivity to depth-dependent variability in bFe because any excess Fe can be efficiently transported to surface waters. This demonstrates that NPP in HNLC areas can be sensitive to the vertical variability in bFe that results from fluctuations in irradiance and temperature. We hypothesize that abiotic processes dictate the depth over which bFe concentrations will be

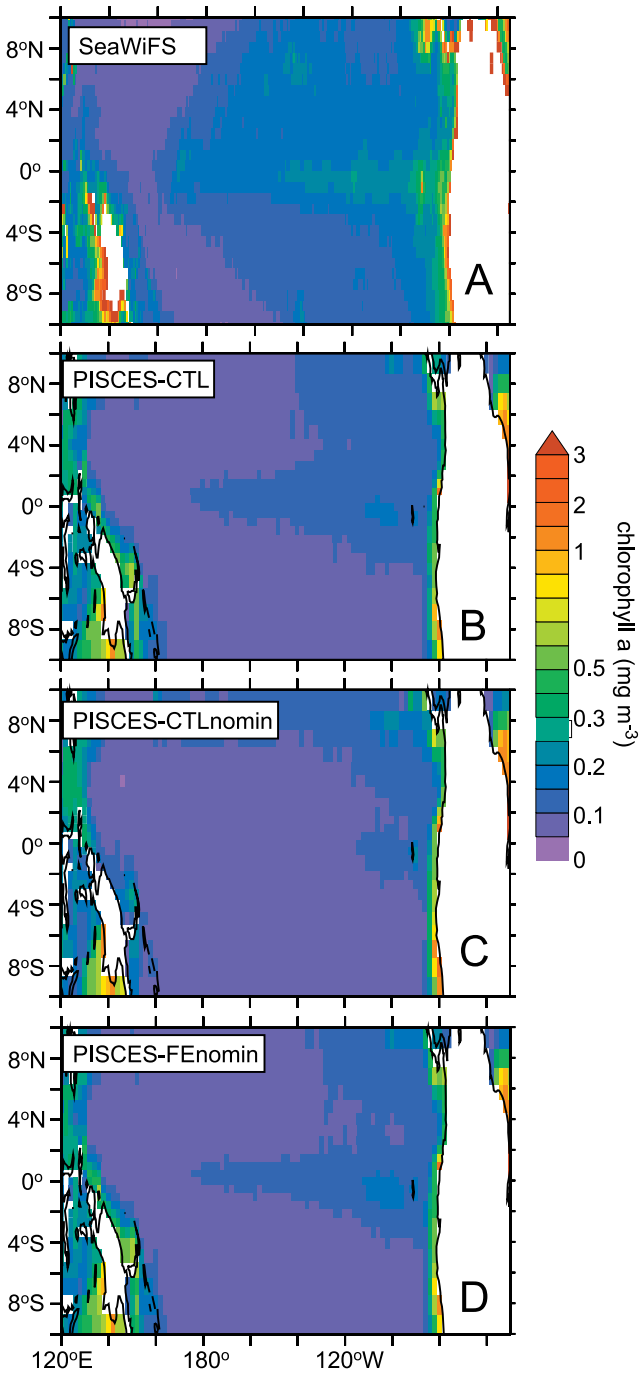

Figure 5. Surface water chlorophyll *a* concentrations (mg m^{-3}) for May from (a) the SeaWiFS climatology (1998–2006, denoted SeaWiFS), (b) the standard Pelagic Integration Scheme for Carbon and Ecosystem studies (PISCES) version with a minimum Fe concentration [*Aumont and Bopp*, 2006] (denoted PISCES-CTL), (c) the standard PISCES version without a minimum Fe concentration (denoted PISCES-CTLnomin), and (d) PISCES without a minimum Fe concentration, but with Fe chemistry (using the results from Figure 2h, denoted PISCES-Fenomin).

sufficient to alleviate Fe limitation of phytoplankton growth. In turn, this determines the physical environment within which phytoplankton can achieve net growth, as well as the efficiency of Fe-based NPP (via the irradiance dependency of Fe/C ratios).

[32] Our results have important implications for the modeling of both future and past ocean biogeochemistry. Current global OBMs typically only include one pool of dFe, accounting for ligand complexation and nonbiogenic losses in a relatively simple fashion [e.g., *Gregg et al.*, 2003; *Dutkiewicz et al.*, 2005; *Aumont and Bopp*, 2006; *Moore and Doney*, 2007] and therefore ignore the role of reactions that are controlled by light and temperature. Although such shortcomings can be overcome for equilibrium simulations by compensatory parameters or processes (e.g., the minimum Fe threshold in PISCES), their absence may prove significant during simulations that consider future changes in the oceans irradiance/mixing regime. For example, climate models suggest that the future ocean will become more stratified [e.g., *Sarmiento et al.*, 2004], which will reduce the upwelling supply of nutrients, including Fe, but will also elevate mixed layer irradiance levels and hence Fe bioavailability. Models utilizing simple parameterizations of seawater Fe chemistry will be unable to account for the role of such processes in governing bFe concentrations and thus the degree of phytoplankton Fe limitation. While understanding the impact of climate change on ocean biogeochemistry will necessitate a holistic consideration of a variety of ocean processes (e.g., changes in vertical nutrient supply and dust deposition, as well as photoadaptation to changing mixed layer irradiance), we would suggest that for a given mixed layer Fe inventory (and for the assumptions inherent in our formulation of abiotic Fe chemistry), greater stratification will elevate bFe/dFe and increase the efficiency of Fe-based NPP (via the reduced Fe demand).

[33] If the physical circulation were to change (as is probable for future or past climates), one would expect NPP to be impacted by the variability in bFe that arises from changes in the light and temperature environment in HNLC regions. However, it is important to note that our approach here only addresses the minimum sensitivity of NPP to Fe chemistry. We do not represent all the degrees of freedom present in the prognostic Fe supply model in PISCES, only the impact of light and temperature on bFe under idealized mixed layer conditions. For example, we find bFe/dFe changes slightly as a function of the tFe concentration, but sensitivity experiments between 0.01 and 5 nM show that variability in bFe/dFe is always <1% of the mean bFe/dFe at a given irradiance and temperature. However, biotic feedbacks, such as the production of Fe binding ligands, are not represented and future global modeling will need to account for the recently observed spatial variability in ligand concentrations [e.g., *Buck and Bruland*, 2007] and possibly also their kinetic characteristics and photolability. Nevertheless, our model will permit the evaluation of the potential importance of abiotic Fe cycling under a changing irradiance/mixing regime. In doing so, it will also be important to consider the impact of any ecosystem response (e.g., changes in phytoplankton physiology, growth strategies, species composition and associated food web

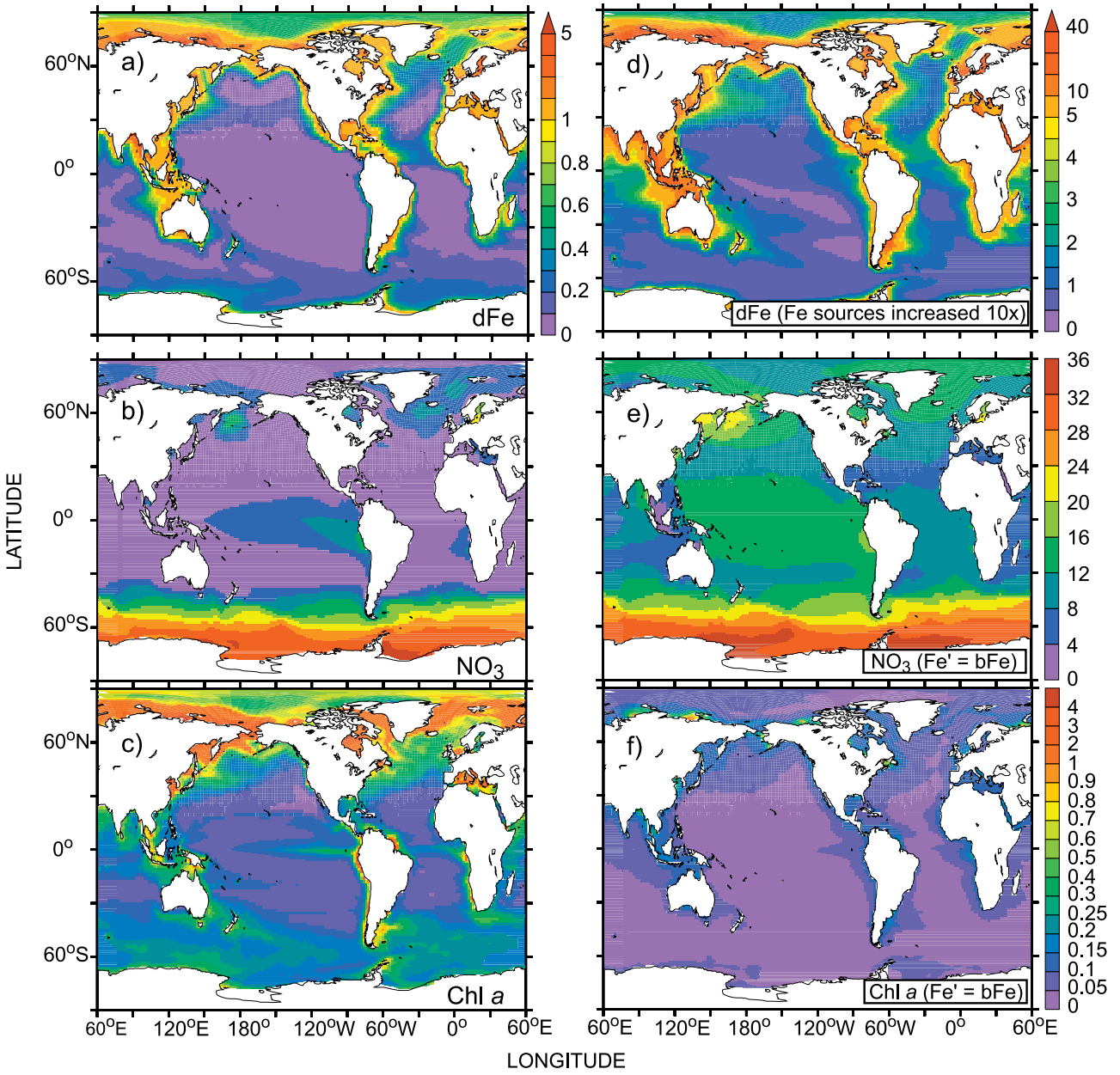

Figure 6. Surface concentrations of annually averaged (a) dissolved Fe (nM), (b) NO_3 (μM), and (c) chlorophyll *a* (mg m^{-3}) when Fe chemistry is included in PISCES as per Figure 2h. (d) Surface water dFe (nM) if sedimentary and atmospheric sources are increased tenfold when Figure 2e drives bFe (please also note the scale change between Figures 2a and 2d). (e and f) Annually averaged chlorophyll *a* (mg m^{-3}) and NO_3 (μM) when only inorganic Fe is assumed to be bioavailable (using the results from Figure 2e).

structure) to physically driven variability in bFe concentrations on biogeochemical cycling in HNLC regions.

5. Summary and Conclusions

[34] Using a relatively complex model of abiotic Fe cycling, we find that the irradiance/mixing regime exerts a strong control on the speciation of Fe and the subsequent supply of bFe to phytoplankton. Although different representations of the Fe cycle result in variability in bFe/dFe, the positive trend with light is robust (for any given Fe model formulation). We find that bioavailable Fe ligands can greatly increase the bFe concentration and highlight the role of light in driving the transfer of Fe from unavailable to bioavailable species. On the other hand, inorganic Fe is highly sensitive to the seawater temperature and can only accumulate in mixed layers that are cold and well lit. For a given irradiance and temperature, bFe/dFe increases with the presence of bioavailable Fe ligands, reduced ligand photolability, greater ligand conditional stability, and increased

ligand concentrations. In our study it was necessary to make certain assumptions regarding abiotic Fe chemistry and more information on variability in abiotic rate processes (Fe(II) oxidation, Fe(III)L photoreduction, ligand complexation/dissociation and Fe(III) precipitation to solids) will help in further constraining the our conclusions.

[35] The influence of the irradiance/mixing regime on bFe is neglected by all contemporary global OBMs, but will be important if we wish to account for the impact of expected changes in the physical structure of the mixed layer on Fe speciation. We outline a means by which the first-order impact of Fe chemistry may be applied to global OBMs and the minimum sensitivity to a variety of Fe cycle formulations be evaluated. We propose that abiotic processes dictate the vertical variability in bFe concentrations and thus the efficiency of Fe-based NPP. It also appears unlikely that only inorganic Fe is limiting to phytoplankton. Further information on the bioavailability, conditional stability and photolability of specific ligand groups, alongside data concerning the irradiance/mixing regime is necessary to better constrain the impact of stratification on the supply of Fe to phytoplankton.

[36] **Acknowledgments.** All simulations were performed at the French National computing center IDRIS. We thank Philip Boyd, Andrew Bowie, Kristen Buck, and two anonymous reviewers for their comments. This research was funded by ANR/GOBAC and grants from the National Science Foundation (grant OPP-9696045), the Ocean Carbon Sequestration Research Program, Biological and Environmental Research (BER), U.S. Department of Energy (grant DE-FG02-04ER63896), and the NASA Oceanography Program (grant NAG5-11264).

References

Aumont, O., and L. Bopp (2006), Globalizing results from ocean in situ iron fertilization studies, *Global Biogeochem. Cycles*, *20*, GB2017, doi:10.1029/2005GB002591.

Barbeau, K., E. L. Rue, K. W. Bruland, and A. Butler (2001), Photochemical cycling of iron in the surface ocean mediated by microbial iron(III)-binding ligands, *Nature*, *413*(6854), 409–413, doi:10.1038/35096545.

Barbeau, K., E. L. Rue, C. G. Trick, K. W. Bruland, and A. Butler (2003), Photochemical reactivity of siderophores produced by marine heterotrophic bacteria and cyanobacteria based on characteristic Fe(III) binding groups, *Limnol. Oceanogr.*, *48*, 1069–1078.

Blain, S., C. Guieu, H. Claustre, K. Leblanc, T. Moutin, B. Queguiner, J. Ras, and G. Sarthou (2004), Availability of iron and major macronutrients for phytoplankton in the northeast Atlantic Ocean, *Limnol. Oceanogr.*, *49*, 2095–2104.

Bopp, L., O. Aumont, P. Cadule, S. Alvain, and M. Gehlen (2005), Response of diatoms distribution to global warming and potential implications: A global model study, *Geophys. Res. Lett.*, *32*, L19606, doi:10.1029/2005GL023653.

Boukhalfa, H., and A. L. Crumbliss (2002), Chemical aspects of siderophore mediated iron transport, *Biometals*, *15*, 325–339, doi:10.1023/A:1020218608266.

Bowie, A. R., et al. (2001), The fate of added iron during a mesoscale fertilization experiment in the Southern Ocean, *Deep Sea Res., Part II*, *48*, 2703–2743, doi:10.1016/S0967-0645(01)00015-7.

Bowie, A. R., E. P. Achterberg, P. N. Sedwick, S. Ussher, and P. J. Worsfold (2002), Real-time monitoring of picomolar concentrations of iron(II) in marine waters using automated flow injection-chemiluminescence instrumentation, *Environ. Sci. Technol.*, *36*, 4600–4607, doi:10.1021/es020045v.

Boyd, P. W., et al. (2000), A mesoscale phytoplankton bloom in the polar Southern Ocean stimulated by iron fertilization, *Nature*, *407*, 695–702, doi:10.1038/35037500.

Boyd, P. W., et al. (2004), The decline and fate of an iron-induced phytoplankton bloom, *Nature*, *428*, 549–553, doi:10.1038/nature02437.

Boye, M., A. Aldrich, C. M. G. van den Berg, J. T. M. De Jong, H. Nirmaier, M. Veldhuis, K. R. Timmermans, and H. J. W. de Baar (2006), The chemical speciation of iron in the north-east Atlantic Ocean, *Deep Sea Res., Part I*, *53*, 667–683, doi:10.1016/j.dsr.2005.12.015.

Buck, K. N., and K. W. Bruland (2007), The physiochemical speciation of dissolved iron in the Bering Sea, Alaska, *Limnol. Oceanogr.*, *52*, 1800–1808.

Buck, K. N., M. C. Lohan, C. J. M. Berger, and K. W. Bruland (2007), Dissolved iron speciation in two district river plumes and an estuary: Implications for riverine iron supply, *Limnol. Oceanogr.*, *52*, 843–855.

Chen, M., R. C. H. Dei, W.-X. Wang, and L. D. Guo (2003), Marine diatom uptake of iron bound with natural colloids of different origins, *Mar. Chem.*, *81*, 177–189, doi:10.1016/S0304-4203(03)00032-X.

Coale, K. H., et al. (1996), A massive phytoplankton bloom induced by an ecosystem-scale iron fertilization experiment in the equatorial Pacific Ocean, *Nature*, *383*, 495–501.

Coale, K. H., R. M. Gordon, and X. Wang (2005), The distribution and behavior of dissolved and particulate iron and zinc in the Ross Sea and Antarctic circumpolar current along 170°W, *Deep Sea Res., Part I*, *52*, 295–318, doi:10.1016/j.dsr.2004.09.008.

Conkright, M. E., S. Levitus, and T. P. Boyer (1994), *World Ocean Atlas 1994*, vol. 1, *Nutrients, NOAA Atlas NESDIS 1*, 150 pp., U.S. Dept. of Comm., NOAA, Washington, D. C.

Croot, P. L., and P. Laan (2002), Continuous shipboard determination of Fe(II) in polar waters using flow injection analysis with chemiluminescence detection, *Anal. Chim. Acta*, *466*, 261–273, doi:10.1016/S0003-2670(02)00596-2.

Croot, P. L., A. R. Bowie, R. D. Frew, M. T. Maldonado, J. A. Hall, K. A. Safi, J. La Roche, P. W. Boyd, and C. S. Law (2001), Retention of dissolved iron and Fe(II) in an iron induced Southern Ocean phytoplankton bloom, *Geophys. Res. Lett.*, *28*(18), 3425–3428, doi:10.1029/2001GL013023.

Cullen, J. T., B. A. Bergquist, and J. W. Moffat (2006), Thermodynamic characterization of the partitioning of iron between soluble and colloidal species in the Atlantic Ocean, *Mar. Chem.*, *98*, 295–303, doi:10.1016/j.marchem.2005.10.007.

de Baar, H. J. W., et al. (2005), Synthesis of iron fertilization experiments: From the iron age in the age of enlightenment, *J. Geophys. Res.*, *110*, C09S16, doi:10.1029/2004JC002601.

Dutkiewicz, S., M. J. Follows, and P. Parekh (2005), Interactions of the iron and phosphorous cycles: A three dimensional model study, *Global Biogeochem. Cycles*, *19*, GB1021, doi:10.1029/2004GB002342.

Emmenegger, L., R. Schonenberger, L. Sigg, and B. Schulzberger (2001), Light-induced redox cycling of iron in circumneutral lakes, *Limnol. Oceanogr.*, *46*, 49–61.

Eppley, R. W. (1972), Temperature and phytoplankton growth in the sea, *Fish. Bull.*, *70*, 1063–1085.

Gledhill, M., and C. M. G. van den Berg (1994), Determination of the complexation of Fe(III) with natural organic complexing ligands in seawater using cathodic stripping voltammetry, *Mar. Chem.*, *47*, 41–54, doi:10.1016/0304-4203(94)90012-4.

Gregg, W. W., P. Ginoux, P. S. Schopf, and N. W. Casey (2003), Phytoplankton and iron: Validation of a global three-dimensional ocean biogeochemical model, *Deep Sea Res., Part II*, *50*, 3143–3169, doi:10.1016/j.dsr2.2003.07.013.

Henderson, G. M., et al. (2007), GEOTRACES: An international study of the global marine biogeochemical cycles of trace elements and their isotopes, *Chem. Erde Geochem.*, *67*, 85–131, doi:10.1016/j.chemer.2007.02.001.

Hudson, R. J. M., and F. M. M. Morel (1990), Iron transport in marine phytoplankton: Kinetics of cellular and medium coordination reactions, *Limnol. Oceangr.*, *35*, 1002–1020.

Hutchins, D. A., A. E. Witter, A. Butler, and G. W. Luther III (1999), Competition among marine phytoplankton for different chelated iron species, *Nature*, *400*, 858–861, doi:10.1038/23680.

Johnson, K. S., R. M. Gordon, and K. H. Coale (1997), What controls dissolved iron concentrations in the world ocean?, *Mar. Chem.*, *57*, 137–161, doi:10.1016/S0304-4203(97)00043-1.

King, D. W., H. A. Lounsbury, and F. J. Millero (1995), Rates and mechanism of Fe(II) oxidation at nanomolar iron concentrations, *Environ. Sci. Technol.*, *29*, 818–824, doi:10.1021/es00003a033.

Macrellis, H. M., C. G. Trick, E. L. Rue, G. Smith, and K. W. Bruland (2001), Collection and detection of natural iron-binding ligands from seawater, *Mar. Chem.*, *76*, 175–187, doi:10.1016/S0304-4203(01)00061-5.

Maldonado, M. T., and N. M. Price (1999), Utilization of iron bound to strong organic ligands by plankton communities in the subarctic Pacific Ocean, *Deep Sea Res., Part II*, *46*, 2447–2473, doi:10.1016/S0967-0645(99)00071-5.

Maldonado, M. T., and N. M. Price (2001), Reduction and transport of organically bound iron by *Thalassiosira oceanica* (Bacillariophyceae), *J. Phycol.*, *37*, 298–309.

Maldonado, M. T., R. F. Strzepek, S. Sander, and P. W. Boyd (2005), Acquisition of iron bound to strong organic complexes, with different Fe binding groups and photochemical reactivities, by plankton communities in Fe-limited subantarctic waters, *Global Biogeochem. Cycles*, *19*, GB4S23, doi:10.1029/2005GB002481.

Maldonado, M. T., A. E. Allen, J. C. Chong, K. Lin, D. Leus, N. Karpenko, and S. Harris (2006), Copper dependent iron transport in coastal and oceanic diatoms, *Limnol. Oceanogr.*, *51*, 1729–1743.

Martin, J. H. (1990), Glacial-interglacial CO_2 change: The iron hypothesis, *Paleoceanography*, *5*, 1–13, doi:10.1029/PA005i001p00001.

Martinez, J. S., G. P. Zhang, P. D. Holt, H. T. Jung, C. J. Carrano, M. G. Haygood, and A. Butler (2000), Self-assembling amphiphilic siderophores from marine bacteria, *Science*, *287*(5456), 1245–1247, doi:10.1126/science.287.5456.1245.

Millero, F. J., S. Sotolongo, and M. Izaguirre (1987), The oxidation kinetics of Fe(II) in seawater, *Geochim. Cosmochim. Acta*, *51*, 793–801, doi:10.1016/0016-7037(87)90093-7.

Moore, J. K., and O. Braucher (2007), Sedimentary and mineral sources of dissolved iron to the World Ocean, *Biogeosci. Discuss.*, *4*, 1279–1327.

Moore, J. K., and S. C. Doney (2006), Remote sensing observations of ocean physical and biological properties in the region of the Southern Ocean iron enrichment experiment (SOFeX), *J. Geophys. Res.*, *111*, C06026, doi:10.1029/2005JC003289.

Moore, J. K., and S. C. Doney (2007), Iron availability limits the ocean nitrogen inventory stabilizing feedback between marine denitrification and nitrogen fixation, *Global Biogeochem. Cycles*, *21*, GB2001, doi:10.1029/2006GB002762.

Morel, F. M. M., and N. M. Price (2003), The biogeochemical cycles of trace metals in the oceans, *Science*, *300*, 944–947, doi:10.1126/science.1083545.

Ozturk, M., et al. (2004), Iron enrichment and photoreduction of iron under UV and PAR in the presence of hydroxycarboxylic acid: Implications for phytoplankton growth in the Southern Ocean, *Deep Sea Res., Part II*, *51*, 2841–2856.

Raven, J. A. (1988), The iron and molybdenum use efficiencies of plant growth with different energy, carbon and nitrogen sources, *New Phytol.*, *109*, 279–287, doi:10.1111/j.1469-8137.1988.tb04196.x.

Reid, R. T., D. G. Live, D. J. Faulkner, and A. Butler (1993), A siderophore from a marine bacterium with an exceptional ferric iron affinity constant, *Nature*, *366*, 455–458, doi:10.1038/366455a0.

Rijkenberg, M. J. A., A. C. Fisher, J. J. Kroon, L. J. A. Gerringa, K. R. Timmermans, H. T. Wolterbeek, and H. J. W. de Baar (2005), The influence of UV irradiation on the photoreduction of iron in the Southern Ocean, *Mar. Chem.*, *93*, 119–129, doi:10.1016/j.marchem.2004.03.021.

Rodgers, K. B., J. L. Sarmiento, O. Aumont, C. Crevoisier, C. de Boyer Montegut, and N. Metzl (2008), A wintertime uptake window for anthropogenic CO_2 in the North Pacific, *Global Biogeochem. Cycles*, *22*, GB2020, doi:10.1029/2006GB002920.

Ryther, J. H. (1956), Photosynthesis in the ocean as a function of light intensity, *Limnol. Oceanogr.*, *1*, 61–70.

Salmon, T. P., A. L. Rose, B. A. Neilan, and T. D. Waite (2006), The FeL model of iron acquisition: Nondissociative reduction of ferric complexes in the marine environment, *Limnol. Oceanogr.*, *51*, 1744–1754.

Sarmiento, J. L., et al. (2004), Response of ocean ecosystems to climate warming, *Global Biogeochem. Cycles*, *18*, GB3003, doi:10.1029/2003GB002134.

Schneider, B., L. Bopp, M. Gehlen, J. Segschneider, T. L. Frölicher, P. Cadule, P. Friedlingstein, S. C. Doney, M. J. Behrenfeld, and F. Joos (2008), Climate-induced interannual variability of marine primary and export production in three global coupled climate carbon cycle models, *Biogeosciences*, *5*, 597–614.

Shaked, Y., A. B. Kustka, and F. M. M. Morel (2005), A general kinetic model for iron acquisition by eukaryotic phytoplankton, *Limnol. Oceanogr.*, *50*, 872–882.

Sunda, W. G., and S. A. Huntsman (1997), Interrelated influence of iron, light and cell size on marine phytoplankton growth, *Nature*, *390*, 389–392, doi:10.1038/37093.

Sverdrup, H. U. (1953), On the conditions for the vertical blooming of phytoplankton, *J. Cons. Cons. Int. Explor. Mer*, *18*, 287–295.

Tagliabue, A., and K. R. Arrigo (2006), Processes governing the supply of iron to phytoplankton in stratified seas, *J. Geophys. Res.*, *111*, C06019, doi:10.1029/2005JC003363.

Tagliabue, A., and L. Bopp (2008), Towards understanding global variability in ocean carbon-13, *Global Biogeochem. Cycles*, *22*, GB1025, doi:10.1029/2007GB003037.

Tagliabue, A., L. Bopp, and O. Aumont (2008), Ocean biogeochemistry exhibits contrasting responses to a large scale reduction in dust deposition, *Biogeosciences*, *5*, 11–24.

Takahashi, T., et al. (2002), Global sea-air CO_2 flux based on climatological surface ocean pCO_2, and seasonal biological and temperature effects, *Deep Sea Res., Part II*, *49*, 1601–1622, doi:10.1016/S0967-0645(02)00003-6.

Timmermans, K. R., B. van der Wagt, and H. J. W. de Baar (2004), Growth rates, half-saturation constants, and silicate, nitrate, and phosphate depletion in relation to iron availability of four large, open-ocean diatoms from the Southern Ocean, *Limnol. Oceanogr.*, *49*, 2141–2151.

Tsuda, A., et al. (2003), A mesoscale iron enrichment in the western subarctic Pacific induces a large centric diatom bloom, *Science*, *300*, 958–961, doi:10.1126/science.1082000.

Weber, L., C. Volker, A. Oschilies, and H. Buchard (2007), Iron profiles and speciation at the Bermuda Atlantic Time-series Study site: A model based sensitivity study, *Biogeosciences*, *4*, 689–706.

Willey, J. D., R. J. Kieber, P. J. Seaton, and C. Miller (2008), Rainwater as a source of Fe(II)-stabilizing ligands to seawater, *Limnol. Oceanogr.*, *53*, 1678–1684.

Witter, A. E., and G. W. Luther III (1998), Variation in Fe-organic complexation with depth in the northwestern Atlantic Ocean as determined using a kinetic approach, *Mar. Chem.*, *62*, 241–258, doi:10.1016/S0304-4203(98)00044-9.

Witter, A. E., D. A. Hutchins, A. Butler, and G. W. Luther III (2000), Determination of conditional stability constants and kinetic constants for strong model Fe-binding ligands in seawater, *Mar. Chem.*, *69*, 1–17, doi:10.1016/S0304-4203(99)00087-0.

Zafiriou, O. C., B. M. Voelker, and D. L. Sedlak (1998), Chemistry of the superoxide radical (O_2^-) in seawater: Reactions with inorganic copper complexes, *J. Phys. Chem. A.*, *102*, 5693–5700.

K. R. Arrigo, Department of Geophysics, Stanford University, Stanford, CA 94305, USA.

O. Aumont, Laboratoire d'Océanographie et de Climatologie: Expérimentation et Approches Numériques, Centre IRD de Bretagne, IPSL, F-29280 Plouzané, France.

L. Bopp and A. Tagliabue, Laboratoire des Sciences du Climat et de l'Environnement, IPSL, CEA, UVSQ Orme des Merisiers, CNRS, Bat 712, F-91198 Gif sur Yvette, France. (alessandro.tagliabue@lsce.ipsl.fr)